33rd Annual International Conference of the IEEE EMBS
Boston, Massachusetts USA, August 30 - September 3, 2011

Noninvasive Reconstruction of the Three-dimensional Ventricular Activation Sequence during Pacing and Ventricular Tachycardia in the Rabbit Heart

Chengzong Han, *Student Member, IEEE,* Steven M. Pogwizd, Cheryl R. Killingsworth, and Bin He, *Fellow, IEEE*

***Abstract*—Ventricular arrhythmias represent one of leading causes for sudden cardiac death, a significant problem in public health. Noninvasive imaging of cardiac electric activities associated with ventricular arrhythmias plays an important role in better our understanding of the mechanisms and optimizing the treatment options. The present study aims to rigorously validate a novel three-dimensional (3-D) cardiac electrical imaging (3-DCEI) technique with the aid of 3-D intra-cardiac mapping during paced rhythm and ventricular tachycardia (VT) in the rabbit heart. Body surface potentials and intramural bipolar electrical recordings were simultaneously measured in a closed-chest condition in thirteen healthy rabbits. Single-site pacing and dual-site pacing were performed from ventricular walls and septum. VTs and premature ventricular complexes (PVCs) were induced by intravenous norepinephrine (NE). The non-invasively imaged activation sequence correlated well with invasively measured counterparts, with a correlation coefficient of 0.72 and a relative error of 0.30 averaged over all paced beats and NE-induced PVCs and VT beats. The averaged distance from imaged site of initial activation to measured site determined from intra-cardiac mapping was ~5mm. These promising results suggest that 3-DCEI is feasible to non-invasively localize the origins and image activation sequence of focal ventricular arrhythmias.**

I. Introduction

VENTRICULAR arrhythmias continue to be a leading cause of death and disability, with more than 400,000 cases of sudden death annually in the US alone. Noninvasive cardiac electric imaging techniques provide a novel means which offers the potential to help define underlying arrhythmia mechanisms (e.g., characterizing the complex activation patterns of ventricular tachycardia (VT)) and to facilitate clinical managements of these arrhythmias (e.g., guiding catheter ablation or implantation of cardiac resynchronization therapy). Efforts have been made to estimate the equivalent cardiac sources from body surface potential maps (BSPMs) by solving the electrocardiographic (ECG) inverse problem, which includes moving dipole solutions [1]-[3], epicardial potential imaging [4]-[6], and heart surface activation imaging [7]-[9].

Imaging cardiac electrical activities throughout the three-dimensional (3-D) myocardium is important considering the fact that arrhythmias typically originate from the subendocardium (and, at times, from intramural sites) [10]. Investigations have been made in imaging the 3-D cardiac electrical activity with the aid of a heart cellular automaton model [11]-[13]. Recently, a physical-model based 3-D cardiac electrical imaging (3-DCEI) approach has been proposed to image ventricular activation sequence from the inversely reconstructed equivalent current densities (ECDs) [14]-[15]. The aim of the present study is to rigorously evaluate the imaging performance of this novel 3-DCEI approach using a well-established 3-D intra-cardiac mapping procedure [16]-[17] in the rabbit heart. Single-site pacing from a number of left ventricle (LV), right ventricle (RV) and septal sites was performed to simulate more realistic single cardiac sources. Simultaneous dual-site pacing was induced to evaluate the capability of 3-DCEI to image more complex cardiac excitation processes. 3-DCEI was also applied to imaging the activation sequence of clinically-relevant VTs and premature ventricular complexes (PVCs) induced by norepinephrine (NE). The 3-DCEI imaged results were quantitatively compared with simultaneous intra-cardiac mapping results and imaging performance was assessed.

II. Methods

A. Rabbit Model and Experimental Procedures

Healthy New Zealand white rabbits were studied under a protocol approved by the Institutional Animal Care and Use Committees of the University of Minnesota and the University of Alabama at Birmingham. Fig. 1 shows a schematic diagram of the experimental protocol. For each rabbit, up to 64 repositionable BSPM electrodes were uniformly placed to cover the anterior-lateral chest up to the mid-axillary line. The heart was exposed via median sternotomy, and up to 27 transmural plunge-needle electrodes were inserted in the LV, RV, and septum. LV and RV electrodes contained 8 bipolar electrode-pairs with an inter-electrode distance of 500 μm [17]. Septal electrodes contained 4 bipolar electrode-pairs separated by 2.5mm. The

Manuscript received April 15, 2011. This work was supported in part by the National Institutes of Health under Grant HL080093 [B.H.], HL073966 [S.M.P], and the National Science Foundation under Grant CBET-0756331 [B.H.]. C.H. was supported in part by a Predoctoral Fellowship from the American Heart Association, Midwest Affiliate.

C. Han (hanxx158@umn.edu) and B. He (binhe@umn.edu) are with the Department of Biomedical Engineering, University of Minnesota, Minneapolis, MN 55455, USA.

S. M. Pogwizd and C. R. Killingworth are with the Department of Medicine, University of Alabama at Birmingham, Birmingham, AL, 35294, USA.

chest and skin were then carefully closed with silk suture, and the mapping electrode wires were externalized above and below the sternotomy incision. Bipolar electrograms were continuously recorded from all electrode-pairs together with body surface potentials from surface electrodes. At the completion of the mapping study, ultra fast computed tomography (UFCT) scans were performed on the living rabbit to construct the realistic heart-torso model and extract the location of BSPM electrodes and plunge-needle electrodes within the myocardium. The rabbit was then euthanized and the plunge-needle electrodes were carefully localized by replacing each with a labeled pin. The heart was then excised and fixed in formalin; a post-operative UFCT scan was performed to further facilitate precise 3-D localization of the transmural electrodes.

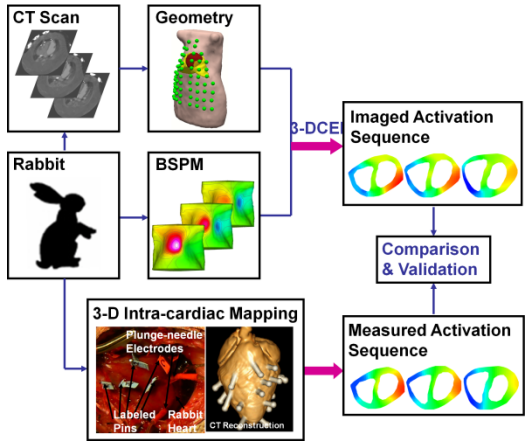

Fig. 1. Schematic diagram of the experimental protocol for validating the 3-dimentional cardiac electrical imaging (3-DCEI) technique with simultaneous measurements from 3-D intra-cardiac mapping.

Rapid single-site pacing and simultaneous dual-site pacing were performed (for 10-20 secs) via bipolar electrode-pairs on selected plunge-needle electrodes in the ventricular myocardium using a specially-designed junction box. NE was infused at 25-100 μg/kg/min (3 minutes at each dose) and ventricular ectopic beats including PVCs and nonsustained monomorphic VTs were induced.

B. *Physical-model Based 3-DCEI Approach*

The physical-model based 3-DCEI approach is developed by modeling 3-D cardiac electrical activities using ECDs and by mathematically solving a spatial-temporal linear inverse problem from BSPMs. For each rabbit, the realistic geometry heart-torso model was constructed from UFCT images using a commercial software package CURRY 6.0 (Compumedics, NC). This heart-torso model was exported for further forward and inverse computation. A distributed ECD model was used to represent the cardiac electrical sources within the 3-D ventricular myocardium. Derived from bidomain theory [18], potentials measurable over the body surface are linearly related to the 3-D ECD distribution using the boundary element method, given a tessellated geometrical heart-torso model and prior knowledge of the electrical conductivities of relevant tissues and organs. A spatiotemporal regularization technique and lead-field normalized weighted minimum norm [19] estimation were used to solve the inverse problem to reconstruct the time course of local ECD at each myocardial site. The activation time at each myocardial site was determined as the instant when the time course of the estimated local ECD reaches its maximum magnitude [15].

C. *3-D Intra-cardiac Mapping*

During 3-D intra-cardiac mapping, the intersection between each transmural needle and the heart surface, and the orientation of each needle within the 3-D ventricular myocardium was determined directly from the same UFCT images used for constructing the detailed heart model after the mapping study. Based on the determined coordinate for the intersection between the needle and the epicardial surface, and the prior structure information (e.g., inter-distance between bipolar electrode-pairs) of the needle, the coordinates of each bipolar electrode-pairs on the plunge needle within the heart model were calculated precisely from epicardium to endocardium using a linear equation. An alternative heart surface model was built from the post-operative UFCT images of the isolated heart with labeled pins (representing the sites of transmural needles), and the location of each needle within this heart surface model was determined from photographs of the isolated heart. This alternative heart surface model was carefully compared with the previous detailed heart model so that the identification and localization of the needles in that detailed heart model could be determined exclusively and precisely. The corresponding activation time of each recording electrode was assigned on the basis of peak criteria [10], [17] and then a weighted average interpolation algorithm was applied to obtain the complete 3-D measured activation sequence throughout the ventricular myocardium.

D. *Statistical Analysis*

The correlation coefficient (CC) and relative error (RE) were computed respectively to quantify the agreement of overall activation pattern and the consistency of the activation time between the invasively measured activation sequence and the non-invasively imaged activation sequence. The localization error (LE) was defined as the distance between site of earliest activation from 3-D intra-cardiac measurements and the center of mass of the myocardial region with the earliest imaged activation time.

III. Results

Thirteen healthy rabbits were studied in the present *in vivo* experiments. The realistic geometry rabbit heart-torso model was constructed for each animal from UFCT images obtained after the mapping study. The rabbit ventricular myocardium was tessellated into 6250±1137 evenly-spaced grid points. The spatial resolution of the ventricle models was 1 mm. There were 178±25 intramural bipolar electrodes during 3-D intra-cardiac mapping and 60±2 BSPM electrodes on the rabbit body surface.

A. *Pacing in the Rabbit Heart*

Simultaneous body surface potential mapping and 3-D intra-cardiac mapping were performed under single-site pacing in nine rabbits. The pacing sites were chosen to cover multiple regions of LV and RV including outflow, apex, lateral, anterior and posterior walls, as well as interventricular septum. The representative comparison between the measured and imaged activation sequence for the single-site pacing is shown in Fig. 2. From the measured activation sequence, it is evident that rabbit was paced at an epicardial LV site in the basal lateral wall. The activation ended in the RV lateral wall. The non-invasively reconstructed activation sequence closely resembled the measured one, with a CC of 0.79 and a RE of 0.31. The initiation of the activation was well localized with a LE of 4.2mm.

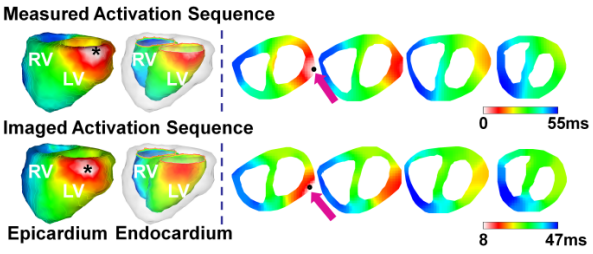

Fig. 2. Comparison between the measured and imaged activation sequences of the single-site pacing in a rabbit heart. In the left column, activation sequence is displayed on epicardial and endocardial surfaces, respectively. In the right column, four axial slices starting from ventricular base are displayed from left to right. The initial sites of activation are marked by asterisks in the left column and a black dot in the right column.

To test the capability of 3-DCEI in imaging more complex cardiac excitation, simultaneous dual-site pacing was performed in five rabbits. Fig. 3 summarizes the results in assessing the ability of the 3-DCEI technique in reconstructing the overall pattern of activation for both the single-site pacing (averaged over 45 pacing locations) and dual-site pacing (averaged over 7 pairs of pacing locations). A slightly better performance of imaging single-site pacing at LV and RV lateral walls was observed in terms of CC and RE, as compared to septum pacing and dual-site pacing. The averaged CC and averaged RE (between non-invasively imaged activation sequence and the one derived from 3-D intra-cardiac mapping) for both single-site pacing and dual-site pacing were 0.73±0.03 and 0.31±0.02 respectively, suggesting excellent agreement of the activation sequence. Furthermore, for single-site pacing, the pacing site was estimated to be 4.9±1.3mm away from the measured one, suggesting reasonable localization accuracy of this approach.

B. *PVCs and VTs in the Rabbit Heart*

Isolated PVCs and nonsustained monomorphic VTs were obtained during the infusion of NE in four rabbits. A total of 28 PVCs and 45 beats of VTs were analyzed and the mechanism of the arrhythmia was defined for all these ventricular ectopic beats from intra-cardiac mapping. All these PVC and VT beats initiated in the subendocardium and did so by a focal, and what we believe to be a nonreentrant mechanism, based on the lack of intervening electrical activity between the preceding beat and the initiation of the ectopic beat in intramural recordings [17]. PVCs in each rabbit demonstrated different initial sites of activation, except one rabbit which had PVCs only initiated from a single site. Seven PVCs initiated in the LV and 21 in the RV. Among these ectopic beats, different activation patterns with different initiation sites were observed. The initiation sites covered both LV and RV, including basal lateral wall, middle lateral wall, and apex.

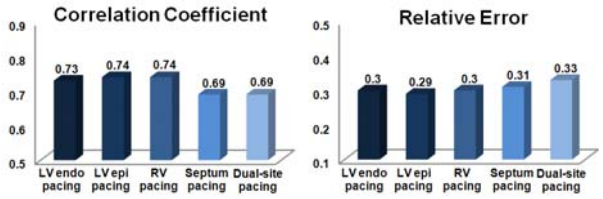

Fig. 3. Summarization of the comparison between the measured and imaged activation sequence for single-site LV, RV, and septum pacing and for dual-site pacing in 13 rabbit hearts.

An example of a representative VT beat in an eight-beat monomorphic VT in a rabbit heart is shown in Fig. 4. After initiation, all VT beats looked similar. As shown in the measured activation sequence in Fig. 4, the VT beat initiated by a focal (nonreentrant) mechanism at the middle lateral wall of anterior RV. After initiation, activation propagated to the LV and terminated at base of LV with a total activation time of 48ms. The imaged activation sequence matched measured activation sequence in its overall activation pattern, with a CC of 0.77 and a RE of 0.31. The initiation of the activation was well localized with a LE of 5.1mm.

IV. Discussion

By comparing the imaged results with simultaneous measurements through 3-D intra-cardiac mapping, the present study has validated the ability of the 3-DCEI approach to identify, localize and resolve single and double electric events during single-site and dual-site paced rhythms, as well as NE-induced nonsustained monomorphic VTs and PVCs in the rabbit heart. Our results showed an excellent agreement of the spatial activation pattern between the non-invasively imaged activation sequence and its directly measured counterpart, as quantified by a CC of 0.72 and a RE of 0.30 averaged over all paced and ectopic beats. The origins of the activation in the imaging results had an averaged distance of ~5mm from the measured sites determined from intra-cardiac mapping. These findings imply that 3-DCEI is feasible in reconstructing the spatial patterns of 3-D ventricular activation sequences, localizing the focal or multiple arrhythmogenic foci, and imaging dynamically changing arrhythmia on a beat-to-beat basis.

The present study has used a novel *in vivo* experimental design in which BSPMs were obtained simultaneously with intramural electrical recordings from plunge-needle electrodes in a closed-chest protocol, and thus provided

quantitative assessments of the 3-DCEI approach. UFCT images were obtained on the anesthetized animals immediately following the mapping studies to accurately model the heart-torso geometry and determine the location of the plunge-needle electrodes within the detailed heart model. The close match between the imaged activation sequence and the direct measurement suggested that significant information regarding ventricular excitation (e.g., activation pattern and regions with earliest and latest activation) has been preserved in the imaged activation maps.

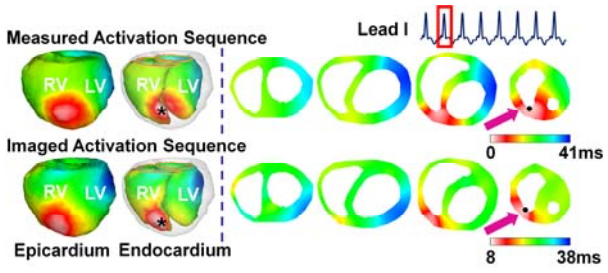

Fig. 4. Comparison between the measured and the imaged activation sequence of an eight-beat monomorphic VT in a rabbit heart.

For the first time, the 3-DCEI approach was applied in imaging activation sequence of ventricular arrhythmia and validated with the aid of invasive 3-D intra-cardiac mapping. NE simulated the activation of the sympathetic nervous system and induced PVC and VT. The measured activation sequence also showed that these arrhythmias usually originated within the subendocardium and may arise from Purkinje cells or subendocardial myocardium. The origins have been well localized by the noninvasive 3-DCEI approach with good accuracy, implying that this approach may be valuable for imaging focal ventricular arrhythmias arising in the deeper myocardium.

The current imaging accuracy is considered to be associated with the inherited errors based on experimental protocol used. Note that the experimental errors are mainly determined by the current procedures and would not linearly scale to the size of the subjects, and thus it shall be reasonable to anticipate that the imaging accuracy would be maintained at the level comparable to rabbit heart (and that would be clinically useful) in species with larger cardiac size. Further validation studies will be needed to assess the imaging accuracy in larger species.

In conclusion, the present study suggests that the 3-DCEI approach can reconstruct 3-D ventricular activation sequence and localize the origin of activation during pacing and focal ventricular arrhythmias, as validated by 3-D intra-cardiac mapping procedure in the rabbit heart. It also suggests the potential application of 3-DCEI as a clinically useful tool to aid in localizing the origins of ventricular arrhythmias and understanding the mechanism of these arrhythmias.

ACKNOWLEDGMENT

The authors are grateful to Drs. Dakun Lai and Chenguang Liu for assistance in data collection and useful discussions.

REFERENCES

[1] Y. Okamoto, Y. Teramachi, and T. Musha, "Limitation of the inverse problem in body surface potential mapping," *IEEE Trans. Biomed. Eng.,* vol. 30, pp. 749-754, Nov. 1983.

[2] R. M. Gulrajani, F. A. Roberge, and P. Savard, "Moving dipole inverse ECG and EEG solutions," *IEEE Trans. Biomed. Eng.,* vol. 31, pp. 903-910, Dec. 1984.

[3] D. M. Mirvis, F. W. Keller, R. E. Ideker, J. W. Cox Jr, R. F. Dowdie, and D. G. Zettergren, "Detection and localization of multiple epicardial electrical generators by a two-dipole ranging technique." *Circ. Res.,* vol. 41, pp. 551-557, Oct. 1977.

[4] R. C. Barr, M. Ramsey, and M. S. Spach, "Relating epicardial to body surface potential distributions by means of transfer coefficients based on geometry measurements," *IEEE Trans. Biomed. Eng.,* vol. 24, pp. 1-11, Jan. 1977.

[5] S. Ghosh, E. K. Rhee, J. N. Avari, P. K. Woodard, and Y. Rudy, "Cardiac memory in patients with Wolff-Parkinson-White syndrome: noninvasive imaging of activation and repolarization before and after catheter ablation," *Circulation,* vol. 118, pp. 907-915,Aug. 2008.

[6] F. Greensite and G. Huiskamp, "An improved method for estimating epicardial potentials from the body surface," *IEEE Trans. Biomed. Eng.,* vol. 45, pp. 98-104, Jan. 1998.

[7] A. J. Pullan, L. K. Cheng, M. P. Nash, C. P. Bradley, and D. J. Paterson, "Noninvasive electrical imaging of the heart: theory and model development," *Ann. Biomed. Eng.,* vol. 29, pp. 817-836, Oct. 2001.

[8] G. Huiskamp and F. Greensite, "A new method for myocardial activation imaging," *IEEE Trans. Biomed. Eng.,* vol. 44, pp. 433-446, Jun. 1997.

[9] B. Tilg, G. Fischer, R. Modre, F. Hanser, B. Messnarz, M. Schocke, C. Kremser, T. Berger, F. Hintringer, and F. X. Roithinger, "Model-based imaging of cardiac electrical excitation in humans," *IEEE Trans. Med. Imaging.,* vol. 21, pp. 1031-1039, Sep. 2002.

[10] S. M. Pogwizd, J. P. McKenzie, and M. E. Cain, "Mechanisms underlying spontaneous and induced ventricular arrhythmias in patients with idiopathic dilated cardiomyopathy," *Circulation,* vol. 98, pp. 2404-2414, Dec. 1998.

[11] G. Li and B. He, "Localization of the site of origin of cardiac Activation by means of a heart-model-based electrocardiographic imaging approach," *IEEE Trans. Biomed. Eng.,* vol. 48, pp. 660-669, Jun. 2001.

[12] B. He, G. Li, and X. Zhang, "Noninvasive imaging of cardiac transmembrane potentials within three-dimensional myocardium by means of a realistic geometry anisotropic heart model," *IEEE Trans. Biomed. Eng.,* vol. 50, pp. 1190-1202, Oct. 2003.

[13] X. Zhang, I. Ramachandra, Z. Liu, B. Muneer, S. M. Pogwizd and B. He, "Noninvasive three-dimensional electrocardiographic imaging of ventricular activation sequence," *Am. J. Physiol.-Heart Circul. Physiol.,* vol. 289, pp. H2724-H2732, Dec. 2005.

[14] B. He and D. Wu, "Imaging and visualization of 3-D cardiac electric activity," *IEEE Trans. Inf. Technol. Biomed.,* vol. 5, pp. 181-186, Sep. 2001.

[15] Z. Liu, C. Liu, and B. He, "Noninvasive reconstruction of three-dimensional ventricular activation sequence from the inverse solution of distributed equivalent current density," *IEEE Trans. Med. Imaging.,* vol. 25, pp. 1307-1318, Oct. 2006.

[16] C. Han, Z. Liu, X. Zhang, S. M. Pogwizd, and B. He, "Noninvasive three-dimensional cardiac activation imaging from body surface potential maps: a computational and experimental study on a rabbit model," *IEEE Trans. Med. Imaging.,* vol. 27, pp. 1622-1630, Nov. 2008.

[17] S. M. Pogwizd, "Nonreentrant mechanisms underlying spontaneous ventricular arrhythmias in a model of nonischemic heart failure in rabbits," *Circulation,* vol. 92, pp. 1034-1048, Aug. 1995.

[18] W. T. Miller, and D. B. Geselowitz, "Simulation studies of the electrocardiogram. I. The normal heart," *Circ. Res.,* vol. 43, pp. 301-315, Aug. 1978.

[19] J. Wang, S. Williamson, and L. Kaufman, "Magnetic source images determined by a lead-field analysis: the unique minimum-norm least-squares estimation," *IEEE Trans. Biomed. Eng.,* vol. 39, pp. 665-675, Jul. 1992.